

A novel method to calculate the mechanical properties of cancer cells based on atomic force microscopy

TIANBIAO ZHANG¹, YING ZHAO², ZHAOXUE TONG¹, YIFU GUAN^{1*}

¹ Department of Biochemistry and Molecular Biology, China Medical University, Shenyang, Liaoning Province, China.

² Department of General Surgery, Shengjing Hospital of China Medical University, Shenyang, Liaoning Province, China.

Purpose: Mechanical properties, as the inherent characteristics of cells, play a critical role in many essential physiological processes, including cell differentiation, migration, and growth. The mechanical properties of cells are one of the criteria that help to determine whether the tissue contains lesions at the single cell level, and it is very important for the early prevention and accurate diagnosis of diseases. Atomic force microscopy (AFM) makes it possible to measure the mechanical properties at single cell level in physiological state. This paper presents a novel method to calculate the mechanical properties of cancer cells more accurately through Atomic force microscopy. *Methods:* A new induced equation of Hertz's model, called differential Hertz's model, has been proposed to calculate the mechanical properties of cancer cells. Moreover, the substrate effect has also been effectively reduced through comparing the calculated mechanical properties of cell at different cell surface areas. *Results:* The results indicate that the method utilized to calculate the mechanical properties of cells can effectively eliminate the errors in calculation, caused by the thermal drift of AFM system and the substrate effect, and thus improve the calculation accuracy. *Conclusion:* The mechanical properties calculated by our method in this study are closer to the actual value. Thus, this method shows potential for use in establishing a standard library of Young's modulus.

Key words: cells' mechanical properties, differential Hertz's model, eliminating thermal drift, AFM, Young's modulus

1. Introduction

The cell is a basic unit of structure, function and biology of all known living organisms, it also contains all life information and general features of life. The in-depth study of the structures and activities of cells is important in all life sciences, because the structures and activities of cells affect many physiological processes including growth, differentiation, development, death and tumor growth [1], [2]. Investigation of the change of mechanical properties of cells is a good way of studying the structures and activities of cells [3]. These mechanical properties can be measured easily through atomic force microscopy (AFM) or other tools, which make the research on structures and activities of cells more convenient and intuitional. In addition, the inherent mechanical properties of cells

make it possible to perceive external mechanical stimulation and transform the stimulation into chemical signals to regulate the physiological activities [4]. And the transmission mechanism would be damaged if cells' structure or mechanical properties change [5], which causes some tissues to for lesions [6]. So, studies on the mechanical properties of cells can contribute to the understanding of the physiological mechanisms, and this allows earlier prevention of diseases [7].

The emergence of the AFM technique [8] makes it possible to observe the ultrastructure of surface of living cells. In AFM, a sharp tip over the sample surface is raster-scan to study sample topography properties. The technique can be used to study physical activities of living cells at nano-scale, as it can be operated in a homologous physiological environment at a nano-spatial resolution level [9]. Previously, some

* Corresponding author: Yifu Guan, Department of Biochemistry and Molecular Biology, China Medical University, No.77 Puhe Road, Shenyang North New Area, Shenyang, Liaoning Province, P.R. China, 110012. Phone number: +86 18511048877, e-mail: tbzhang@mail.cmu.edu.cn

Received: January 13th, 2015

Accepted for publication: May 9th, 2015

relevant studies on measuring mechanical properties of cells utilizing AFM have been carried out and many results have been achieved. Mechanical properties of the living rat liver macrophages have been measured by AFM in physiological buffer to investigate the contribution of cytoskeleton to the mechanical properties of cells [10]. In addition, the mechanical properties of L929 cells have also been measured and the results have provided evidence of the existence of mechanical coupling between the cell membrane and the cytoskeleton [11]. Moreover, the mechanical properties of cancerous cells and normal cells have also been measured, and the results showed that the cancerous cells can be distinguished from the normal ones by analyzing the differences of their mechanical properties acquired by AFM [12], [13]. However, in all of these studies, the application of the AFM technique involved the use of a small and sharp tip, which was harmful to the cells. Moreover, the measured mechanical properties of cells only represented partial points on the cells. In order to measure mechanical properties of the entire cell, a spherical tip was fabricated through connecting a microsphere to the AFM tip [14], [15]. The method increased the contacting area between the probe of AFM and the cells, which reduced the damage caused to the cells. However, the mechanical properties measured using the spherical probe still contains only several scatter points or a very small region and are not representative of the mechanical properties of the entire cell.

In this paper, a novel approach has been proposed to measure the mechanical properties of cells based on a new induced equation of Hertz's model, called differential Hertz's model, which can help to obtain the mechanical properties at almost covering all area of the cell surface. In addition, considering the thermal drift of AFM system and the substrate effect, which impacted the accuracy of re-imaging sample surface, a new method to eliminate the thermal drift and substrate effect was proposed, respectively.

2. Materials and methods

2.1. Atomic force microscopy

The AFM consists of a cantilever with a sharp tip at the end, scanners, position sensitivity detector (PSD), controller and others, as shown in Fig. 1. When the tip approaches to a sample surface, forces between the tip and the sample surface lead to a de-

flexion of the cantilever according Hooke's law, where the forces include mechanical contact force, van der Waals' force, etc. Simultaneously, the deflection results in a change of PSD signals, which are generated through a reflected laser spot from the top of the cantilever. So, when the AFM tip raster scans the sample surface, the sample topographic properties are acquired through converting the PSD signals into desired signals via controller.

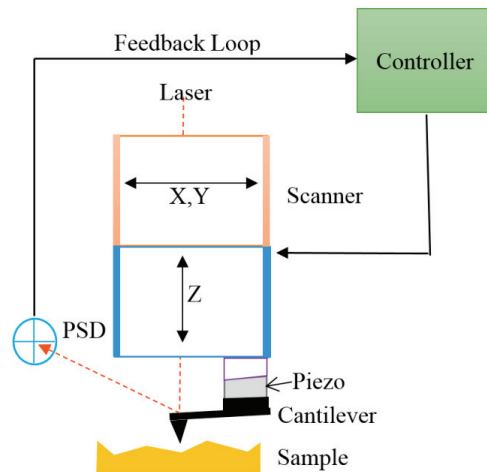


Fig. 1. The schematic diagram of AFM

2.2. Differential Hertz's model

One of the common methods to analyze the mechanical properties of cells is to calculate Young's modulus of cells, which is the essential characteristic of cells. And the widely used method to calculate Young's modulus is the Hertz's model, which approximates the sample as an isotropic and linear elastic solid occupying an infinitely extending half space [16]–[18]. Hertz's model is formulated as follows.

For a spherical tip

$$\mathbf{F} = \frac{4}{3} \frac{E}{(1-\nu^2)} \sqrt{R} \delta^{3/2}, \quad (1)$$

where F denotes the applied loading force to cause the deformation (δ) of the cell, E is Young's modulus, ν is Poisson's ratio of the sample, and R is the radius of the sphere tip. Equation (1) is such that F with respect to δ , due to the parameters of E , ν and R are all constants, so, Young's modulus can be calculated when the loading force F and δ are measured directly utilizing AFM. Furthermore, there is an assumption for Hertz's model that the tip is not deformation and no extra force exists between the tip and the cell. Moreover, the cell is regarded as an isotropic sphere, so that Poisson's ratio is set at 0.5, and the deforma-

tion of the cell must be set too small to satisfy better the limitation condition of Hertz's model [19].

The deformation of the cell is determined by the deformation of the cantilever (d) and the displacement of piezo (z) in the vertical orientation, as shown in Fig. 2, and the relationship is formulated as follows

$$z = d + \delta. \quad (2)$$

For the applied loading force F and deformation of cantilever d , there is the following equation based on Hooke's law, where k denotes the elasticity coefficient

$$F = kd. \quad (3)$$

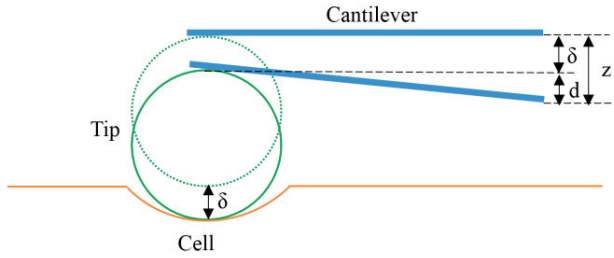


Fig. 2. The sketch of deformation when the tip is applied onto the cell surface

In the traditional methods used to calculate Young's modulus utilizing Hertz's model, the vital problem is to find the contact point from the displacement z and the force F curves, where the contact point is position where the tip is first exposed to the cell surface. This would lead to an inevitable error because the point was determined through visual observation [20].

Therefore, in order to measure the mechanical properties of the entire cell, a differential Hertz's model has been proposed. Assuming that \mathbf{F}_1 and \mathbf{F}_2 are the applied loading forces into the deformation of cell δ_1 and δ_2 in the same desired area of cell surface, respectively. And the corresponding displacements of piezo are z_1 and z_2 , respectively. At first, equation (1) is transformed to the following equation

$$\delta = \left[\frac{3(1-\nu^2)\mathbf{F}}{4E\sqrt{R}} \right]^{\frac{2}{3}}. \quad (4)$$

Then, the differential Hertz's model is formulated as the following equation

$$\delta_1 - \delta_2 = \left[\frac{3(1-\nu^2)\mathbf{F}}{4E\sqrt{R}} \right]^{\frac{2}{3}} \left(\mathbf{F}_1^{\frac{2}{3}} - \mathbf{F}_2^{\frac{2}{3}} \right). \quad (5)$$

So, Young's modulus can be calculated by the following equation

$$\mathbf{E} = \frac{3(1-\nu^2)}{4\sqrt{R}} \left(\frac{\mathbf{F}_1^{\frac{2}{3}} - \mathbf{F}_2^{\frac{2}{3}}}{\delta_1 - \delta_2} \right)^{\frac{3}{2}}. \quad (6)$$

Here, the force \mathbf{F} can be measured using AFM based on equation (7), and the displacement of piezo can also be measured directly. Thus, the method used to calculate Young's modulus can help to avoid the error of finding contact point. And then Young's modulus of the cell can be calculated as the averages of \mathbf{E} .

$$\mathbf{F} = k \cdot S_c \cdot \mathbf{D}. \quad (7)$$

Here, S_c denotes the cantilever sensitivity (m/V) and \mathbf{D} is the deflection (V) of applied loading force measured by AFM directly.

In other words, the procedures for calculating Young's modulus utilizing AFM based on the differential Hertz's model are briefly described as follows. Firstly, the same region of the sample surface is imaged twice with different deflections caused by the applied loading force; simultaneously, the deflections and height images are recorded. Secondly, a suitable area of sample surface is selected in two images and the corresponding deflections and height information are determined. Finally, Young's modulus is calculated based on the differential Hertz's model using the deflection and height information.

2.3. Method of eliminating thermal drift of the AFM system

There inevitably exists an uncertainty error caused by the thermal drift of the AFM system, which affects the precision of calculating Young's modulus in our study. This leads to an absence of no complete overlap for two sample topography images acquired by scanning twice via AFM at different loading forces. Moreover, the deviation of the tip position during acquiring an image also contributes negatively. So, how to eliminate the error caused by the thermal drift is very important to improve the calculation accuracy. The vital step to eliminate the thermal drift error is calibration. In this paper, a method of calibrating error caused by the thermal drift of AFM system has been proposed and the procedure is described as follows.

Firstly, the same region of the sample is repeatedly imaged at a fixed time interval (t) with a fixed deflection.

Secondly, the same feature points in all images are selected, respectively, and the coordinates (absolute

coordinate system) are calculated in corresponding image, as shown in Fig. 3.

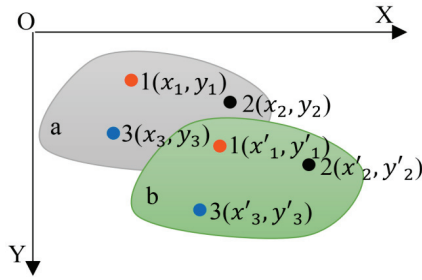


Fig. 3. The method of calibration of thermal drift. “a” denotes the first image and “b” denotes the second image, and circles are the feature points

Finally, assuming that the coordinates of the feature points in both images are (x_i, y_i) and (x'_i, y'_i) , where $i = 1, 2, \dots, n$, respectively, the calibration of the thermal drift was performed using the following equation

$$\text{At the } X \text{ axis: } cx_i = \frac{1}{n} \sum_{i=1}^n (x_i - x'_i), \quad (8)$$

$$\text{At the } Y \text{ axis: } cy_i = \frac{1}{n} \sum_{i=1}^n (y_i - y'_i). \quad (8)$$

Equations (8) and (9) are used to calculate the error caused by the thermal drift of the AFM system at adjacent time points in the horizontal and the vertical orientations, respectively. Then, the relationship curve between the error of the thermal drift and the time can be established using the errors at the fixed interval calculated based on equations (8) and (9). The slope of the curve is the thermal drift error at unit time.

To realize the complete overlap of both morphology images, the second image should compensate the thermal drift error with the calibration, which will guarantee the accuracy of calculating Young's modulus using the differential Hertz's model.

2.4. Cell culture

The cells used in our study were human embryonic kidney 293 (HEK293) cells, which is a specific cell line originally derived from human embryonic kidney cells grown in tissue culture. And the HEK293 cells were cultured in Dulbecco's modified Eagle's medium (DMEM, Thermo Scientific) with 1% penicillin/streptomycin (Thermo Scientific) and 10% fetal

bovine serum (ExCell Bio) solution at 5% ambient CO₂ at 37 °C in a 60 mm culture flask for 24 hours.

3. Results

The prerequisite for the measurement of Young's modulus of cells using the differential Hertz's model is to acquire the sample surface morphology of the same region twice at different loading forces. However, a complete overlap of the measurement region is difficult to obtain when performing the scanning twice, due to the uncertainty error caused by the thermal drift of the AFM system. In addition, the thermal drift is a cumulative error, that is, it is proportional to time. In addition, the error significantly affected the accuracy of the calculated Young's modulus. Therefore, in order to eliminate the error, the thermal drift error was calibrated firstly.

To calibrate the thermal drift error, the desired sample surface was repeatedly scanned with the same scanning parameters of the AFM system (Dimension 3100 AFM, Veeco Inc.) at a certain time. In this experiment, the area was scanned four times at the time period of 5 minutes and the scanning parameters were set as follows: scale 50 μm , rate 1 Hz, lines 512 at room temperature. Then, 8 feature points were selected in each topographic image, as shown in Fig. 4a–d. The relative deviation of each feature point in two adjacent topographies was calculated, and averages of all the distance of all feature points were also calculated. The results of the relationship between the drift distance and the time are shown in Fig. 5. Based on the results, it is asserted that the thermal drift is in direct proportion to the time and the calibration of the thermal drift errors in the horizontal and vertical orientations were calculated as $cx = 0.084 \mu\text{m}/\text{min}$ and $cy = 0.087 \mu\text{m}/\text{min}$, respectively.

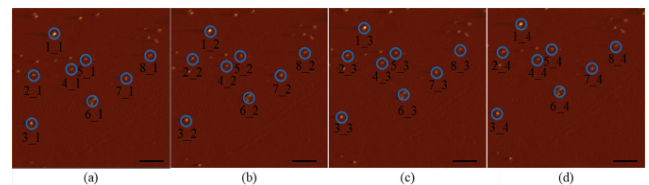


Fig. 4. The calibration of thermal drift. (a)–(d) are the sample surface morphology of the same region at every 5 minutes. The blue circles denote the feature points. The number i_j ($i = 1, 2, 3, 4, 5, 6, 7, 8, j = 1, 2, 3, 4$) indicates feature points at corresponding picture, where i denotes the number of feature while j is the corresponding picture acquired in different time period. The bar is 5 μm

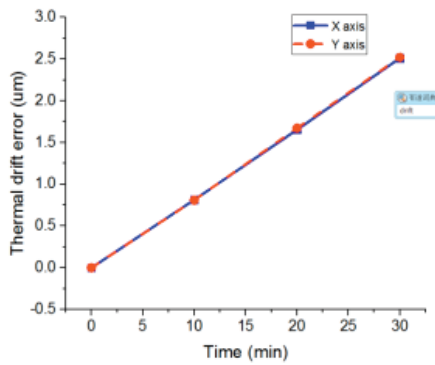


Fig. 5. The curve of thermal drift error versus the time

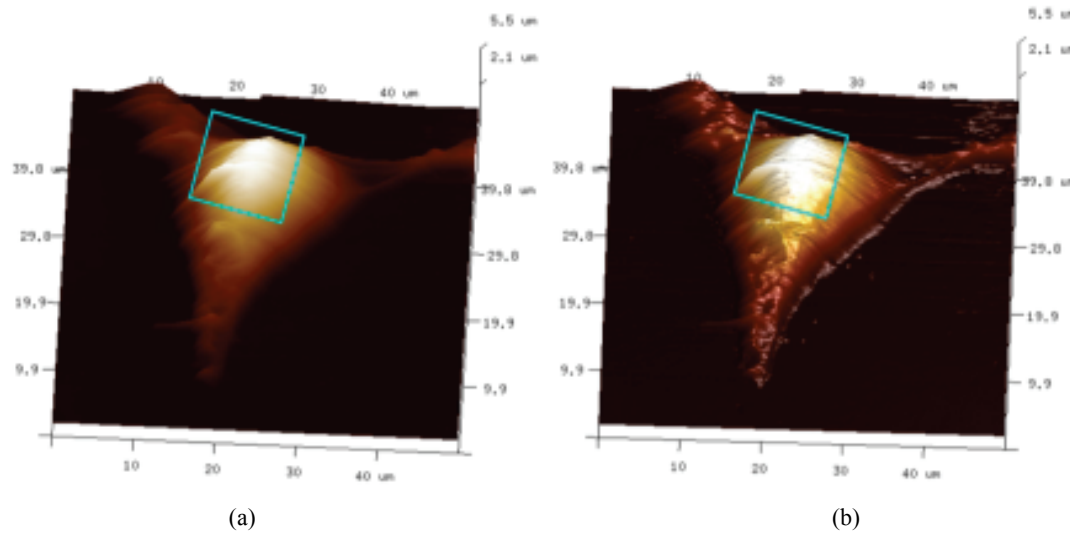


Fig. 6. The sample topographies for calculating Young's modulus. The boxes denote the area selected to calculate Young's modulus

To calculate Young's modulus using the differential Hertz' model, two images should be acquired at different loading forces at firstly, as shown in Fig. 6. A rectangular area with the center of the highest point of the cell was then selected to calculate Young's modulus. Here, it needs to be noted that the position of the second box must be compensated with the thermal drift error.

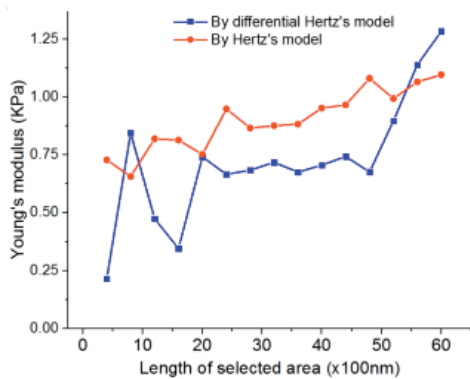


Fig. 7. The curves of Young's modulus calculated by differential Hertz's model and regular Hertz's model versus the length of selected area

Moreover, the selected area should be as far away from the substrate as possible to reduce the substrate effect on the results. The relationship between the sizes of the selected area and the calculated Young's modulus is shown in Fig. 7. From Fig. 7, we concluded that when the length of selected area, which was the size of the box in Fig. 6, was in a smaller region, then the calculated Young's modulus showed more instability, because of the smaller samples used to be calculated; while when it was in a larger region, then the effect from substrate was larger, so that the calculated Young's modulus was increasing with

length. Therefore, a moderate length that allows Young's modulus to be stably calculated was chosen, and Young's modulus of the HEK-293 cell was calculated as 0.7045 ± 0.0011 KPa by the differential Hertz's model. While Young's model calculated by regular Hertz's model showed more instability and gradually increased with length because of the existence of substrate effect, and Young's model is 0.8997 ± 0.1673 KPa. Young's modulus calculated by the Hertz's model is larger than that calculated by this new model, because the latter method reducing the error caused by the substrate effect. And the calculate error was also larger due to the effects of finding contact points and the thermal drift.

4. Discussion

The mechanical properties of cells play an important role in physiological processes, and they are regarded as an indicator of cellular states that can be

used for the early prevention and diagnosis of diseases at a single cell level. The prerequisite condition for achieving these goals is to guarantee accuracy in the calculation of the mechanical properties acquired using AFM. The most important factors that hinder the accuracy of measurement of the mechanical properties of cells include the thermal drift error, the substrate effect error and contact point error. In detail, the thermal drift error is caused by the non-linear creep of piezoceramics of the AFM system and the experimental environment; the substrate effect error is caused by the interaction between the substrates in the culture dish and the cell, and it is in direct proportion to the height and the deformation of cells whose properties are to be measured; and the contact point error is inevitably produced in the procedure of finding the contact point through visual observation.

In this study, we successfully managed to improve the accuracy of measurement of the mechanical properties of cells by eliminating these errors. For the thermal drift error, the error is firstly calibrated and then reduced effectively by compensating the calibration. To reduce the influence of the error caused by the substrate effect, we calculated Young's modulus at different regions on the cell surface and summarized the relationship curve between the calculated Young's modulus and the size of regions. We then averaged the calculated Young's modulus corresponding to the range of the smallest fluctuation of the curve, because the smaller region will show instability and the larger region is affected obviously by the substrate effect. In addition, for the last one, a differential Hertz's model was built to avoid the error caused by finding the contact point based on visual observations. The model can be used to accurately calculate Young's model of a large cell surface area, which can be more accurately represented to Young's model of the entire cell.

However, in order to utilize Young's modulus for the disease diagnosis, more data items of Young's modulus for different cells are necessary, which can be obtained in future studies.

Acknowledgement

This work was supported by a grant from foundation project of science and technology of Liaoning province (Grant No. 2013225021). And there was no specific grant or any funding from others.

References

[1] MOGILNER A., KEREN K., *The Shape of Motile Cells*, *Curr. Biol.*, 2009, 19, 762–771.

- [2] KILIAN K.A., BUGARIJA B., LAHN B.T., MRKSICH M., *Geometric cues for directing the differentiation of mesenchymal stem cells*, *P. Natl. Acad. Sci. USA*, 2010, 107, 4872–4877.
- [3] VOGEL V., SHEETZ M., *Local force and geometry sensing regulate cell functions*, *Nat. Rev. Mol. Cell. Bio.*, 2006, 7, 265–275.
- [4] JANMEY P.A., MCCULLOCH C.A., *Cell mechanics: Integrating cell responses to mechanical stimuli*, *Ann. Rev. Biomed. Eng.*, 2007, 9, 1–34.
- [5] LIM C.T., ZHOU E.H., QUEK S.T., *Mechanical models for living cells – A review*, *J. Biomech.*, 2006, 39, 195–216.
- [6] LI Q.S., LEE G.Y.H., ONG C.N., LIM C.T., *AFM indentation study of breast cancer cells*, *Biochem. Biophys. Res. Commun.*, 2008, 374, 609–613.
- [7] LEE G.Y.H., LIM C.T., *Biomechanics approaches to studying human diseases*, *Trends Biotechnol.*, 2007, 25, 111–118.
- [8] BINNIG G., QUATE C.F., GERBER C., *Atomic Force Microscope*, *Phys. Rev. Lett.*, 1986, 56, 930–933.
- [9] MULLER D.J., DUFRENE Y.F., *Atomic force microscopy: a nanoscopic window on the cell surface*, *Trends Cell. Biol.*, 2011, 21, 461–469.
- [10] ROTSCH C., BRAET F., WISSE E., RADMACHER M., *AFM imaging and elasticity measurements on living rat liver macrophages*, *Cell. Biol. Int.*, 1997, 21, 685–696.
- [11] WU H.W., KUHN T., MOY V.T., *Mechanical properties of 1929 cells measured by atomic force microscopy: Effects of anticytoskeletal drugs and membrane crosslinking*, *Scanning*, 1998, 20, 389–397.
- [12] CROSS S.E., JIN Y.S., RAO J., GIMZEWSKI J.K., *Nanomechanical analysis of cells from cancer patients*, *Nat. Nanotechnol.*, 2007, 2, 780–783.
- [13] MULLER D.J., DUFRENE Y.F., *Atomic force microscopy as a multifunctional molecular toolbox in nanobiotechnology*, *Nat. Nanotechnol.*, 2008, 3, 261–269.
- [14] OBERLEITHNER H., CALLIES C., KUSCHE-VIHRIG K., SCHILLERS H., SHAHIN V., RIETHMULLER C. et al., *Potassium softens vascular endothelium and increases nitric oxide release*, *P. Natl. Acad. Sci. USA*, 2009, 106, 2829–2834.
- [15] NIKKHAH M., STROBL J.S., SCHMELZ E.M., AGAH M., *Evaluation of the influence of growth medium composition on cell elasticity*, *J. Biomech.*, 2011, 44, 762–766.
- [16] CARL P., SCHILLERS H., *Elasticity measurement of living cells with an atomic force microscope: data acquisition and processing*, *Pflugers Archiv, European Journal of Physiology*, 2008, 457, 551–559.
- [17] DARLING E.M., TOPEL M., ZAUSCHER S., VAIL T.P., GUILAK F., *Viscoelastic properties of human mesenchymally-derived stem cells and primary osteoblasts, chondrocytes, and adipocytes*, *J. Biomech.*, 2008, 41, 454–464.
- [18] TOUHAMI A., NYSTEN B., DUFRENE Y.F., *Nanoscale mapping of the elasticity of microbial cells by atomic force microscopy*, *Langmuir*, 2003, 19, 4539–4543.
- [19] COSTA K.D., *Single-cell elastography: Probing for disease with the atomic force microscope*, *Dis. Markers*, 2003, 19, 139–154.
- [20] LI M., LIU L.Q., XI N., WANG Y.C., DONG Z.L., XIAO X.B. et al., *Atomic force microscopy imaging and mechanical properties measurement of red blood cells and aggressive cancer cells*, *Sci. China Life Sci.*, 2012, 55, 968–973.